AIP | Applied Physics Letters

Electrostatic self-aligned placement of single nanodots by protein supramolecules

Shigeo Yoshii, Shinya Kumagai, Kazuaki Nishio, Ayako Kadotani, and Ichiro Yamashita

Citation: Applied Physics Letters **95**, 133702 (2009); doi: 10.1063/1.3236524
View online: http://dx.doi.org/10.1063/1.3236524
View Table of Contents: http://scitation.aip.org/content/aip/journal/apl/95/13?ver=pdfcov
Published by the AIP Publishing

Electrostatic self-aligned placement of single nanodots by protein supramolecules

Shigeo Yoshii,[1] Shinya Kumagai,[1,a)] Kazuaki Nishio,[1] Ayako Kadotani,[2] and Ichiro Yamashita[1,2,3,b)]
[1]*ATRL, Panasonic Corporation, 3-4 Hikaridai, Seika, Kyoto 619-0237, Japan*
[2]*CREST, Japan Science and Technology, 4-1-8 Honcho, Kawaguchi, Saitama 332-0012, Japan*
[3]*Graduate School of Materials Science, Nara Institute of Advanced Science and Technology, 8916-5 Takayama, Ikoma, Nara 630-0101, Japan*

(Received 28 April 2009; accepted 20 August 2009; published online 1 October 2009)

Electrostatic self-aligned positioning of a single 7 nm nanoparticle in the cage-shaped protein ferritin onto an aminosilane disk pattern as large as next-generation photolithography can produce is demonstrated. Genetic modification of the ferritin increased its surface charge density and therefore improved its electrostatic interaction. Single molecules of the recombinant ferritin could achieve self-aligned placement on 32–45 nm disks under the optimal solution condition, which was calculated by numerical analysis. This biological self-aligned placement, incorporated into next-generation photolithography techniques, will be a useful wafer-scale nanofabrication tool. © *2009 American Institute of Physics*. [doi:10.1063/1.3236524]

Producing homogeneous nanoparticles (NPs) and positioning them at designated positions on a substrate, especially silicon (Si), is one of the fundamental requirements for making nanodot-based devices. We have used a biological method to fulfill this requirement. In a previous work, we reported that the cage-shaped protein supramolecule ferritin, which can synthesize an inorganic 7 nm NP inside its cavity,[1–7] can serve as a vehicle to deliver NPs using electrostatic interactions.[8,9] Even though electrostatic interaction is a long-range force and has been assumed to be inappropriate for handling molecules at nanometric scales, precise numeric calculation made it possible to design a pathway through which a negatively charged ferritin adsorbed only onto a positively charged 15 nm 3-aminopropyltriethoxysilane (APTES) disk formed on a negatively charged silicon dioxide (SiO_2) surface. Steric hindrance prevented the adsorption of a second ferritin molecule. The percentage of APTES disks that had a single ferritin molecule was 60%–70%. Heat treatment left only the iron oxide NP at the position where the APTES disk had been. In our present work, we incorporated a self-aligning mechanism into this biological method. Genetic modification of the outer surface of ferritin improved the single ferritin molecule placement on the larger APTES disks that will be produced routinely by emerging next-generation photolithography technology.

Next-generation photolithography techniques such as immersion double patterning will produce structures as small as 32–45 nm at low cost. Therefore, we set the target as self-aligned single ferritin adsorption onto 32–45 nm APTES disks. We first tried an experiment adsorbing Fer8, which we have used in a previous work,[7] onto 32–45 nm APTES disks on a SiO_2 surface under several conditions. Fer8 has a zeta potential of −14.7 mV at 0.1 mM ionic strength (IS). The circular symmetry of the attractive and repulsive force produced by an APTES disk and SiO_2 surface should guide a ferritin molecule to the center of the disk and the negative charges on the ferritin should repel the adsorption of a second ferritin molecule.[10] However, the results showed multiple adsorptions and the number of ferritin molecules on one disk varied considerably, which apparently indicated that the APTES disk could not provide a narrow electrostatic guideway to the disk and that the force by the first adsorbed ferritin was not strong enough to repel subsequent molecules.

To solve these problems, we increased the negative charge on the ferritin surface via genetic engineering. Increased negative charge strengthens electrostatic attractive and repulsive interactions, which should guide the ferritin molecule more powerfully and precisely. The first ferritin molecule will repel subsequent ferritin molecules more completely (Fig. 1). We surveyed the surface exposed residues of Fer8, and mutated the Fer8 DNA sequence in plasmid pMK2 to substitute the 98th residue (lysine), the 157th residue (glycine), the 159th residue (glutamate), or both the 98th and 105th lysine residues with negatively charged glutamic acid residue. The *E. coli* NovaBlue was transformed with the plasmid. The mutants were named Fer8-K98E, Fer8-G157E, Fer8-Q159E, and Fer8-K98E-K105E. Figure 2 shows the

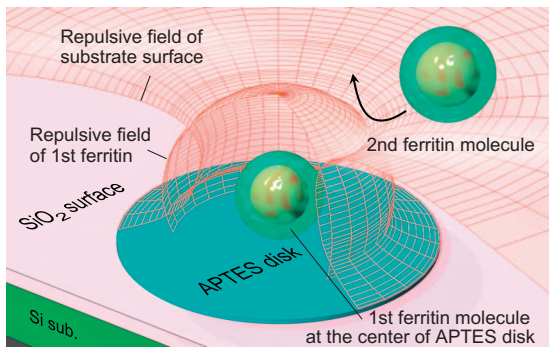

FIG. 1. (Color) Schematic drawing of single ferritin molecule adsorption onto large APTES disk. A second ferritin molecule approaching the APTES disk should be blocked by the repulsive fields of the substrate surface and of the first ferritin molecule, which is located at the center of the disk.

a)Present address: Dept. of Advanced Science and Technology, Toyota Technological Institute, 2-12-1 Hisakata, Tenpaku-ku, Nagoya 468-8511, Japan.
b)Electronic addresses: yamashita.ichiro@jp.panasonic.com and ichiro@ms.naist.jp.

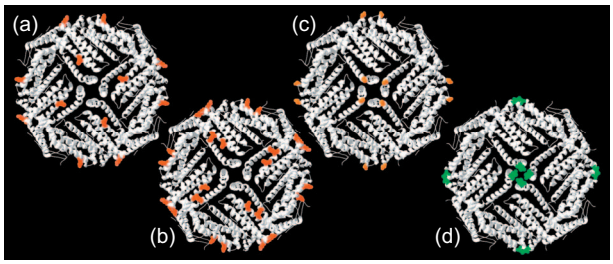

FIG. 2. (Color) Crystal structure of Fer8 showing mutation sites of charge-enhanced ferritin molecules (ribbon model). Colored spheres denote residues, which were substituted with glutamic acid in (a) Fer8-K98E, (b) Fer8-K98E-K105E, (c) Fer8-G157E, and (d) Fer8-Q159E.

sites of amino acid residue replacements. The 98th and 105th residues are located in the region between the threefold and fourfold axes and are fairly evenly distributed. The 157th and 159th residues are located in the vicinity of the fourfold axis.

The mutant ferritins were overproduced and purified as in previous work.[7] The obtained mutants were observed by transmission electron microscopy (TEM) and it was confirmed that all the molecules were hollow cages with the same outer and inner diameters as the original Fer8. Iron oxide cores were biomineralized in the cavities of the purified mutant proteins.[11] Unfortunately, Fer8-Q159E underwent heavy precipitation during the biomineralization process. Highly concentrated additional negative charges at the fourfold axis might have attracted positive iron ions and prompted iron oxide mineralization outside the ferritin, finally causing coprecipitation. After biomineralization, the Fer8-K98E, Fer8-G157E, and Fer8-K98E-K105E were thoroughly purified and TEM observation confirmed the accommodation of iron oxide cores.

The zeta potentials of mutants were measured to evaluate their surface charges (Table I).[12] The charge densities of all mutants were negatively higher than that of the original Fer8 as expected. It is reasonable that the negative charge increase in Fer8-K98E, compared to Fer8, was two times more than that for Fer8-G157E because the positive lysine was replaced in Fer8-K98E, whereas the neutral glycine was replaced in Fer8-G157E. However, the double mutant Fer8-K98E-K105E, which theoretically should have more charges than Fer8-K98E, had lower negative charge density. The reason for this is not clear. Excessive negative charges that are close together might change the local conformation of the protein or might capture positive iron ions on the surface. Based on these experimental results, we used Fer8-K98E in the following analysis and experiments.

We numerically analyzed the three-dimensional terrain of the total protein-substrate interaction energy assuming a 32 nm APTES disk on a Si substrate to find appropriate conditions for placement of a single ferritin molecule. The electrostatic potential distribution was calculated with the Poisson–Boltzmann equation.[8,9] The interaction potential was evaluated as a change in the total free energy.[13,14] The

TABLE I. Surface charge densities of Fer8 and charge-enhanced mutants with iron oxide cores in 0.1 mM MES/Tris buffer (pH 7).

Type of ferritin	Fer8	Fer8-G157E	Fer8-K98E	Fer8-K98E-K105E
Charge density (C cm^{-2})	-2.0×10^{-7}	-3.1×10^{-7}	-4.0×10^{-7}	-3.7×10^{-7}

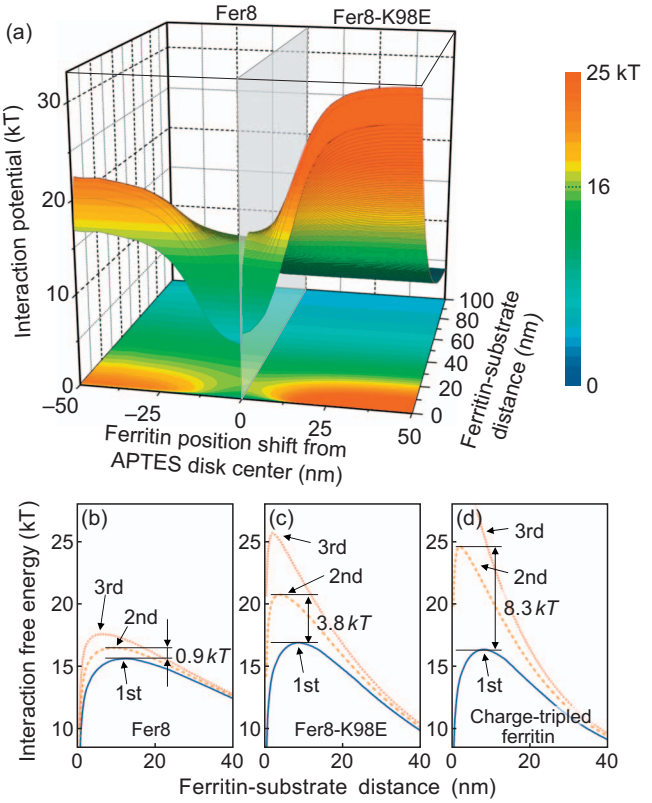

FIG. 3. (Color) (a) Interaction-potential distributions above 32 nm APTES disks. The left half of the figure shows the potential surface for Fer8 at 0.01 mM IS while the right half shows that for Fer8-K98E at 0.1 mM IS. The calculated potential profiles for the first to third adsorptions are shown for (b) Fer8, (c) Fer8-K98E, and (d) charge-tripled ferritin.

surface charge densities of proteins were assumed to be constant, and that of the SiO_2 was calculated with a surface dissociation model at IS from 0.01 to 0.1 mM.[15]

The IS was selected such that the energy of the saddle point of the potential surface was 16 kT, which is presumed to be the maximum barrier height that the ferritin can surmount to reach the substrate surface.[8,12,16] It was set at 0.01 and 0.1 mM (Debye lengths of 96 and 30 nm) for Fer8 and Fer8-K98E, respectively. Figure 3(a) shows the calculated interaction potential distributions. The shape of the interaction potential valley through which ferritin adsorbs is broad for Fer8 [Fig. 3(a), left], while it became much narrower for Fer8-K98E [Fig. 3(a), right]. The barrier height above the APTES disk edge (16 nm from the center) for Fer8 is 2.5 kT higher than that above the disk center (16 kT) and for Fer8-k98E, the value increased threefold to 7.8 kT. This result indicates that the possibility of adsorption at the disk center is greatly increased by the charge enhancement. The lateral component of the potential surface slope above the disk edge, which corresponds to the force toward the disk center, is approximately 2.8 times higher for Fer8-K98E than that for Fer8. The enhanced force guides Fer8-K98E much more powerfully toward the center of the disk during the adsorption process.[10,17] This steep funnel shape of the potential forms a tightly confined path for the ferritin to progress along and the first ferritin molecule is anticipated to achieve self-aligned central adsorption.

We also analyzed the interaction potential for adsorption of a second ferritin molecule by simply assuming the charges in the first ferritin on the APTES disk had diffused uniformly on the disk. Figures 3(b)–3(d) show the calculated interac-

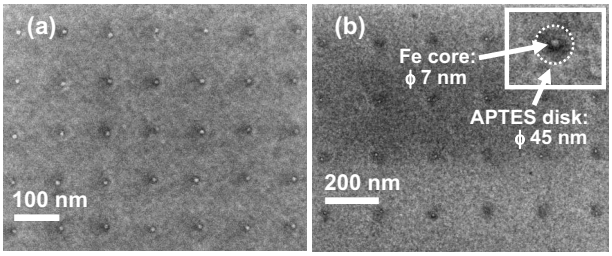

FIG. 4. SEM images of single-molecule placement of charge-enhanced ferritin Fer8-K98E. Single molecules of Fer8-K98E were placed on (a) 32 nm APTES disks at 0.1 mM IS and (b) 45 nm APTES disks at 0.01 mM IS.

tion energy profiles for original Fer8, Fer8-K98E, and a hypothetical ferritin with tripled charge, respectively, when they approach an APTES disk along a vertical line from the disk center. The increases in potential barrier height on the adsorption path due to the adsorption of the first ferritin molecule were 0.9, 3.8, and 8.3 kT for Fer8, Fer8-K98E, and charge-tripled ferritin, respectively. This means 41% ($\sim e^{-0.9}$) of the approaching Fer8 could reach the disks that already have one ferritin, while only 2% ($\sim e^{-3.8}$) of Fer8-K98E could. Changes in IS from optimal value have little effect on the result. Therefore, enhanced charge on ferritin is essential for the single ferritin adsorption.

Our simulation of Fer8 adsorption showed that the single-molecule adsorption ratio, the ratio of disks with a single ferritin molecule to all disks, was smaller than 60% under ideal conditions and that multiple adsorption was inevitable. This result is consistent with the abovementioned experimental result. On the other hand, the single-molecule adsorption ratio for Fer8-K98E could exceed 90% and the multiple-molecule adsorption ratio could be suppressed to less than 5%. If the negative charge on the ferritin is tripled, the single adsorption ratio should further increase up to 99%.

Using the charge-enhanced mutant Fer8-K98E and following the simulation, we conducted adsorption experiments on larger APTES disks. We fabricated 32–45 nm APTES disks on a SiO_2 surface with electron beam lithography, and vapor-phase APTES deposition.[18] Interdisk distances were set to 100–200 nm, which were larger than Debye lengths employed in adsorption. We placed a 0.5 mg/ml solution of ferritin with an iron oxide core in a MES/Tris (pH 7) buffer with a designed IS of 0.1 or 0.01 mM on a prepared substrate for 1 min at room temperature. The samples were then rinsed with pure water and spin dried. After these procedures, surfaces were observed with a scanning electron microscope (SEM, JSM-7400F) at 5.0 kV. Figure 4(a) shows the obtained image. Each of the 32 nm APTES disks arranged in a grid pattern had one Fer8-K98E even though the area of the disk is seven times larger than the cross section of the molecule. No adsorption on the SiO_2 surface was observed. The single-molecule adsorption ratio exceeded 90% and the multiple adsorption ratio was 4.2%, which is consistent with the simulation results. Based on further numerical analysis for 45 nm disks, IS was set at 0.01 mM, which made the saddle point potential of 16 kT,[8,9] and single Fer8-K98E adsorption onto these larger disks was also realized [Fig. 4(b)].

These results showed that electrostatic interaction can place a single NP on a larger APTES disk in a self-aligned manner. There are reports on selective adsorption by other methods such as hydrophobic/philic interactions or surface-specific recognition of peptide aptamers,[19–21] but a few on self-alignment with them.[22] It is hard for short-range interactions to realize self-aligned placement. Automatic single-molecule adsorption on a pattern larger than the molecule is a definite advantage of electrostatic interaction and is due to the nature of its long-range force.

We demonstrated the placement of single 7 nm NPs onto 32–45 nm charged disks by charge-enhanced mutant ferritin. Next-generation photolithographic techniques will produce disks of this size easily and this technique could place single NPs at designated positions easily and economically. Further improvements in the placement of single NPs should be achievable by additional enhancement in the negative charge on the ferritin surface. The use of electrostatic interaction and genetically designed proteins shown in this work could serve as a production tool to position nanodots, which will be used in a variety of applications, such as the nanoetching masks for nanocolumns or nanodisks[23] and as catalyst NPs for forming carbon nanotubes or for low temperature growth of poly-Si films.[24]

The authors thank Mr. Hidenori Tanaka for technical help and Dr. Jonathan Heddle for critical reading. This study was partially supported by Leading Project of MEXT, Japan.

[1] I. Yamashita, Thin Solid Films **393**, 12 (2001).
[2] I. Yamashita, J. Hayashi, and M. Hara, Chem. Lett. **33**, 1158 (2004).
[3] T. Douglas and M. Young, Nature (London) **393**, 152 (1998).
[4] M. Okuda, K. Iwahori, I. Yamashita, and H. Yohimura, Biotechnol. Bioeng. **84**, 187 (2003).
[5] R. Tsukamoto, K. Iwahori, M. Muraoka, and I. Yamashita, Bull. Chem. Soc. Jpn. **78**, 2075 (2005).
[6] K. Yoshizawa, K. Iwahori, K. Sugimoto, and I. Yamashita, Chem. Lett. **35**, 1192 (2006).
[7] K. Iwahori, K. Yoshizawa, M. Muraoka, and I. Yamashita, Inorg. Chem. **44**, 6393 (2005).
[8] S. Kumagai, S. Yoshii, K. Yamada, N. Matsukawa, I. Fujiwara, K. Iwahori, and I. Yamashita, Appl. Phys. Lett. **88**, 153103 (2006).
[9] S. Kumagai, S. Yoshii, K. Yamada, N. Matsukawa, K. Iwahori, and I. Yamashita, Jpn. J. Appl. Phys., Part 1 **45**, 8311 (2006).
[10] H.-W. Huang, P. Bhadrachalam, V. Ray, C.-U. Kim, and S. J. Koh, Appl. Phys. Lett. **93**, 073110 (2008).
[11] S. Yoshii, K. Yamada, N. Matsukawa, and I. Yamashita, Jpn. J. Appl. Phys., Part 1 **44**, 1518 (2005).
[12] J. N. Israelachivili, *Intermolecular and Surface Forces*, 2nd ed. (Academic, New York, 1992).
[13] M. Manciu and E. Ruckenstein, Langmuir **19**, 1114 (2003).
[14] S. Bhattacharjee and M. Elimelech, J. Colloid Interface Sci. **193**, 273 (1997).
[15] J. A. Davis, R. O. James, and J. O. Leckie, J. Colloid Interface Sci. **63**, 480 (1978).
[16] A. Sharma, S. N. Tan, and J. Y. Waltz, J. Colloid Interface Sci. **190**, 392 (1997).
[17] L.-C. Ma, R. Subramanian, H.-W. Huang, V. Ray, C.-U. Kim, and S. J. Koh, Nano Lett. **7**, 439 (2007).
[18] S. Kumagai, S. Yoshii, K. Yamada, I. Fujiwara, N. Matsukawa, and I. Yamashita, J. Photopolym. Sci. Technol. **18**, 495 (2005).
[19] K. Sano, K. Ajima, K. Iwahori, M. Yudasaka, S. Iijima, I. Yamashita, and K. Shiba, Small **1**, 826 (2005).
[20] I. Yamashita, H. Kirimura, M. Okuda, K. Noshio, K.-I. Sano, K. Shiba, T. Hayashi, M. Hara, and Y. Mishima, Small **2**, 1148 (2006).
[21] T. Hayashi, K.-I. Sano, K. Shiba, Y. Kumashiro, K. Iwahori, I. Yamashita, and M. Hara, Nano Lett. **6**, 515 (2006).
[22] S. G. Rao, L. Huang, W. Setyawan, and S. Hong, Nature (London) **425**, 36 (2003).
[23] T. Kubota, T. Hashimoto, Y. Ishikawa, S. Samukawa, A. Miura, Y. Uraoka, T. Fuyuki, M. Takeguchi, K. Nishioka, and I. Yamashita, Appl. Phys. Lett. **89**, 233127 (2006).
[24] H. Kirimura, Y. Uraoka, T. Fuyuki, M. Okuda, and I. Yamashita, Appl. Phys. Lett. **86**, 262106 (2005).